Structure and magnetic properties of Fe-Co nanowires in self-assembled arrays

Qingfeng Zhan, Ziyu Chen,* Desheng Xue, and Fashen Li
Key Laboratory for Magnetism and Magnetic Materials of the Ministry of Education, Lanzhou University, Lanzhou 730000, China

Henry Kunkel, Xuezhi Zhou, Roy Roshko, and Gwyn Williams
Department of Physics and Astronomy, the University of Manitoba, Canada R3T 2N2

(Received 21 May 2001; revised manuscript received 17 December 2001; published 31 October 2002)

Arrays of $Fe_{1-x}Co_x$ ($0.0 \leqslant x \leqslant 1.0$) nanowires have been fabricated by codepositing Fe and Co into porous anodic alumina. Transmission electron microscope results show that the nanowires are regular and uniform, about 7.5 μm in length and 20 nm in diameter. Structural determination by x-ray diffraction indicates that bcc(α), fcc(γ), and hcp(ε) Fe-Co phases appear with variation in composition. However, the phase boundaries are different from that in bulk Fe-Co alloys. Magnetic hysteresis loops measured at temperatures ranging from 5 K to 300 K demonstrate that the arrays of nanowires exhibit uniaxial magnetic anisotropy which is dependent on the shape of each individual nanowire. With increasing Co content, the coercivity of the nanowire arrays, with the magnetic field applied parallel to the wire, first increases and then reaches a maximum value before decreasing. The behavior is interpreted using a magnetization reversal model based on ''chains of spheres'' and the symmetric fanning mechanism.

DOI: 10.1103/PhysRevB.66.134436 PACS number(s): 75.50.Bb, 61.46.+w, 81.15.Pq

I. INTRODUCTION

Recently, electrodeposited magnetic nanowires and their arrays have attracted much attention for their distinctive properties and potential applications. From the point of view of applications, they appear possible for ultrahigh-density magnetic recording media.[1–3] The magnetic recording density in conventional longitudinal recording is typically less than 50 Gb/in.^{2}, the limit determined by thermal instability.[4] However, arrays of magnetic nanowires have the potential to produce a recording density in excess of 100 Gb/in.^{2}.[5] A further point of technological importance is that anodization of aluminum is a cheap process for the synthesis of a nm-scale porous structure. Magnetic materials can be electrodeposited into the pores by ac electrodeposition. Recently, ferromagnetic Fe (Refs. 5 and 6), Co (Refs. 5 and 7), Ni (Refs. 8 and 9), and Fe-Ni (Ref. 10 and Co-Ni (Ref. 11) alloy nanowires have been studied. However, Fe-Co nanowires have, to date, not been investigated. Fe-Co bulk alloys are important magnetic materials due to both a high saturation magnetization and Curie temperature, parameters that cannot be matched by any other alloy system. Fe-Co alloys are mainly used as soft magnetic materials[12,13] due to their relatively low coercive field. By contrast, arrays of nanowires exhibit both a high coercive field and a high squareness ratio resulting from shape anisotropy; they make arrays of Fe-Co nanowires potentially useful for high-density magnetic recording.

Generally, the coercive field and squareness ratio depend on the magnetization reversal process. Consequently the magnetization reversal process in arrays of nanowires has attracted much attention.[14,15] While the chains-of-spheres model with a fanning mechanism has succeeded in describing the behavior of elongated single-domain particles,[16,17] it is difficult to prepare a system of elongated single-domain particles. Currently, chains of iron and cobalt particles have been fabricated by both a chemical method[15] and by electron-beam lithography.[14] These preparation methods are not only rather difficult but the aspect ratios of the samples are also not high enough, so the coercivity is much lower than the value predicted by the chains-of-spheres model of Jacobs and Bean. We have found that one-dimensional nanowires can provide samples with high aspect ratios, so that these arrays of nanowires display much higher coercivity and squareness. Furthermore, not only can nanowires of many kinds of materials be fairly easily synthesized by the electrochemical method, but also the diameter and length of the nanowires be easily controlled. Here we compare experimental results for the nanowires with the chains-of-spheres model and use these model predictions to discuss the magnetization reversal process in these nanowires.

II. EXPERIMENT

The arrays of $Fe_{1-x}Co_x$ ($0.0 \leqslant x \leqslant 1.0$) nanowires have been prepared by coelectrodepositing Fe and Co into anodic aluminum oxide (AAO) templates. The preparation of the AAO templates has been described elsewhere in detail.[5,6] In the process of preparing AAO templates, the Al foils (99.999%) were anodized at 15 v (dc) for 1 h in 1.2 m H_2SO_4 aqueous solution at 20 °C, using the Al foil as the cathode. The Fe and Co atoms were electrodeposited into the AAO templates from an aqueous bath containing $FeSO_4 \cdot 7H_2O$, $CoSO_4 \cdot 7H_2O$, HBO_3, and ascorbic acid. The compositions of the $Fe_{1-x}Co_x$ nanowires were adjusted by varying the Fe^{2+}: Co^{2+} ion ratio in the baths. The pH value of the electrolyte was maintained at about 3.0. The electrodepositions were all conducted at 200 Hz and 15 v (ac) for a duration of 5 min, using graphite as the counter-electrode. The AAO films filled with nanowires were removed from the Al substrates using aqueous $HgCl_2$. The nanowires were liberated from the AAO film by dissolving the alumina layer with aqueous NaOH.

Structural characterizations were performed by means of

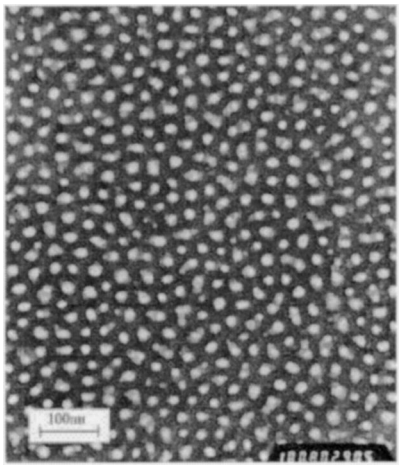

FIG. 1. TEM image of an AAO film with average pore size of about 20 nm.

x-ray diffraction (XRD) using a Rigaku D/Max-2400 diffractometer with Cu $K\alpha$ radiation, and the atomic percentages of Fe and Co in the nanowires were obtained by atomic absorption spectroscopy (AAS). The morphology of the AAO films and the regularity of spacing of nanowires were monitored by transmission electron microscopy (TEM) using a JEOL 2000× microscope operating at 75–100 kV. The magnetic properties of the arrays were investigated using a Quantum Design model 6000 magnetometer (PPMS).

III. RESULTS AND DISCUSSION

A TEM image of an AAO template prepared as mentioned above is shown in Fig. 1. This indicates that the average size of the pores is about 20 nm, while the pore density in the AAO film is about 4.16×10^{11}/in.^{2}. If each nanowire could record a bit cell of information, then the AAO film filled with magnetic nanowires could achieve theoretical bit densities exceeding 400 Gb/in.^{2}.

Figure 2 shows a representative TEM image of two intertwined nanowires which are about 20 nm in diameter and 7.5 μm in length. The corresponding aspect ratio of the nanowires is approximately 375. As the same conditions were used to prepare AAO templates and to electrodeposit all samples, nanowires of different compositions are assumed to be approximately the same size. A bright and a dark field image of a group of nanowires are shown in Fig. 3. Here it can be seen that the nanowires are both regularly spaced and uniform in size. The dark field image shows that the nanowires are not single crystal, but rather resemble a chain of dots. This can be understood as due to a growth process that is not continuous; specifically the depositional reaction only occurs in the negative half cycle of the ac electrodeposition process. According to micromagnetic calculations, the critical radius for single-domain formation is 8.4 and 11.4 nm for isolated Fe and Co particles,[18] respectively. Normally, the critical radius of a sphere in a long chain is much bigger than that of an isolated particle because of the interaction between the spheres, as reported by Martin *et al.*[14] The radius of the spheres comprising the nanowires can be approximated to

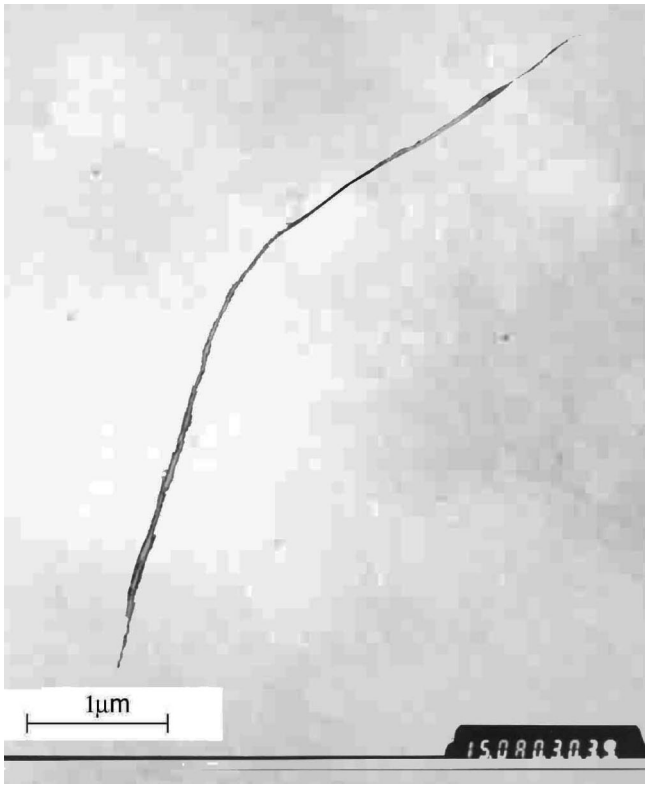

FIG. 2. TEM image of two intertwined Fe-Co nanowires with length about 7.5 μm.

the radius of the pore ($\sim$10 nm) in the AAO film; consequently, it is reasonable to assume that all of the $Fe_{1-x}Co_x$ nanowires are chains of single-domain spheres.

In Fig. 4 the concentration of Co in these $Fe_{1-x}Co_x$ nanowires (obtained by AAS) is plotted against the ionic fraction of Co^{2+} in the electrolyte. The sum of the Fe^{2+} and Co^{2+} ion fractions in the solution is set to unity. Such linear behavior in the codeposition of Fe^{2+} and Co^{2+} ions is not obvious. Since Co is less electronegative than Fe, the depositional velocity of Co is slightly higher than that of Fe. Thus, the concentration of Co in these nanowires is slightly higher than the concentration of Co^{2+} in the corresponding solution, which is consistent with the results in deposited Fe-Co films.[19] Using this relationship (Fig. 4), it is easy to obtain $Fe_{1-x}Co_x$ nanowires of any desired alloy composition

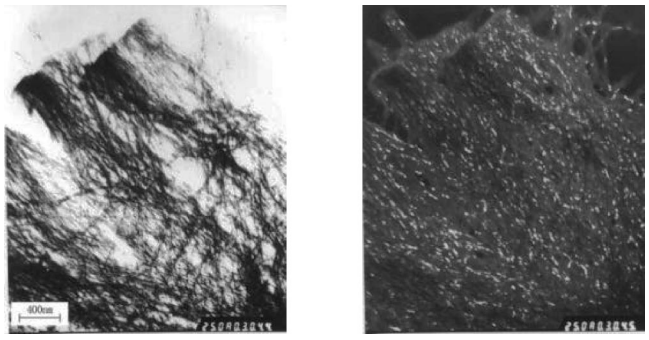

FIG. 3. The bright field and dark field TEM images of a bunch of Fe-Co nanowires.

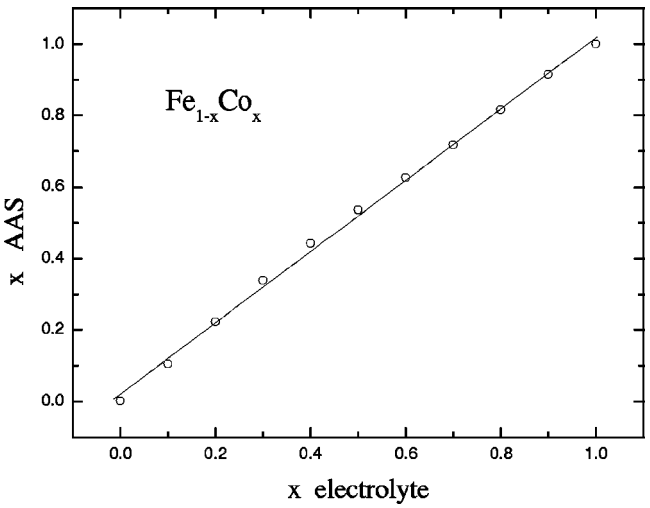

FIG. 4. Plot of the concentration of Co atomic fraction obtained by AAS against the ionic fraction of Co^{2+} in the electrolyte. Solid line is a least-squares fit to the data.

simply by choosing the appropriate atomic proportion of the metals in the aqueous sulfated solutions.

The x-ray diffraction patterns of AAO films filled with $Fe_{1-x}Co_x$ nanowires are shown in Fig. 5. These patterns indicate clearly a texture in the deposited AAO films. All $Fe_{1-x}Co_x$ nanowires with $x \leqslant 0.82$ have a body-centered-cubic (bcc) structure with a [110]-preferred orientation.

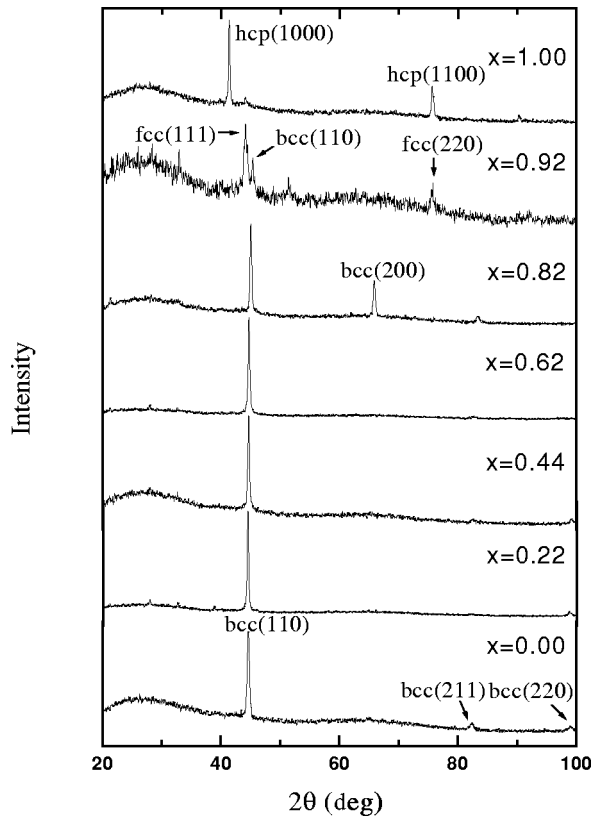

FIG. 5. X-ray diffraction patterns of AAO films filled with $Fe_{1-x}Co_x$ nanowires of various compositions obtained using Cu $K\alpha$ radiation.

TABLE I. The XRD data for the $Fe_{1-x}Co_x$ nanowires. d is the average interplanar spacing along the preferred orientation.

x	0.00	0.22	0.44	0.62	0.82	0.92	1.00
(hkl)	(110)	(110)	(110)	(110)	(110)	(111)	(1000)
d(Å)	2.027	2.033	2.025	2.022	2.011	2.049	2.181

$Fe_{1-x}Co_x$ nanowires with a small amount of Fe—$x=0.92$, for example—exhibit a mixture of bcc and face-centered-cubic (fcc) structures with a [111]-preferred orientation. When $x>0.92$, a cubic- to hexagonal-close-packed (hcp) structural transition occurs. Pure Co in a AAO film exhibits an hcp structure with a [1000]-preferred orientation. Thus the phase transitions in Fe-Co nanowires are similar to these in bulk Fe-Co alloys; however, the phase boundary in nanowires is different from that in the bulk.[20] The $\alpha \rightarrow \gamma$ transition in $Fe_{1-x}Co_x$ nanowires occurs between $x=0.82$ and 0.92, and the $\gamma \rightarrow \varepsilon$ transition occurs between $x=0.92$ and 1.00; in bulk Fe-Co alloys the stable structures at room temperature and below are bcc for 0%–73% cobalt and fcc for 73%–92% cobalt. As is also well known, for Co fine particles, the γ phase appears with an average particle size below 40 nm. Co fine particles with particle size below 20 nm are of pure fcc structure.[21] By contrast, the Co nanowires with diameter $\sim$20 nm have no γ phase present, because the length is in the μm scale. Table I shows XRD data for the $Fe_{1-x}Co_x$ nanowires. The values of the lattice parameter d are slightly larger than these of bulk alloys[20] of the same composition, which means that the lattices in nanowires are expanded in comparison with the bulk.

We have measured the hysteresis loops of the $Fe_{1-x}Co_x$ nanowires in self-assembled arrays with AAO film support at room temperature and 5 K. Figure 6 shows two typical hysteresis loops for the $Fe_{0.38}Co_{0.62}$ sample at 300 K, here $\mathbf{H}(\|)$

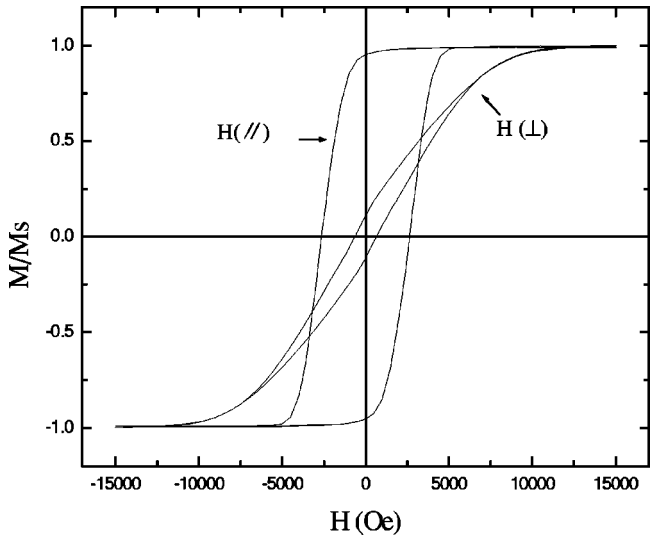

FIG. 6. The hysteresis loops of the $Fe_{0.38}Co_{0.62}$ AAO film at 300. $\mathbf{H}(\|)$ indicates that the applied field is parallel to the nanowires; $\mathbf{H}(\perp)$ indicates that the applied field is perpendicular to the nanowires.

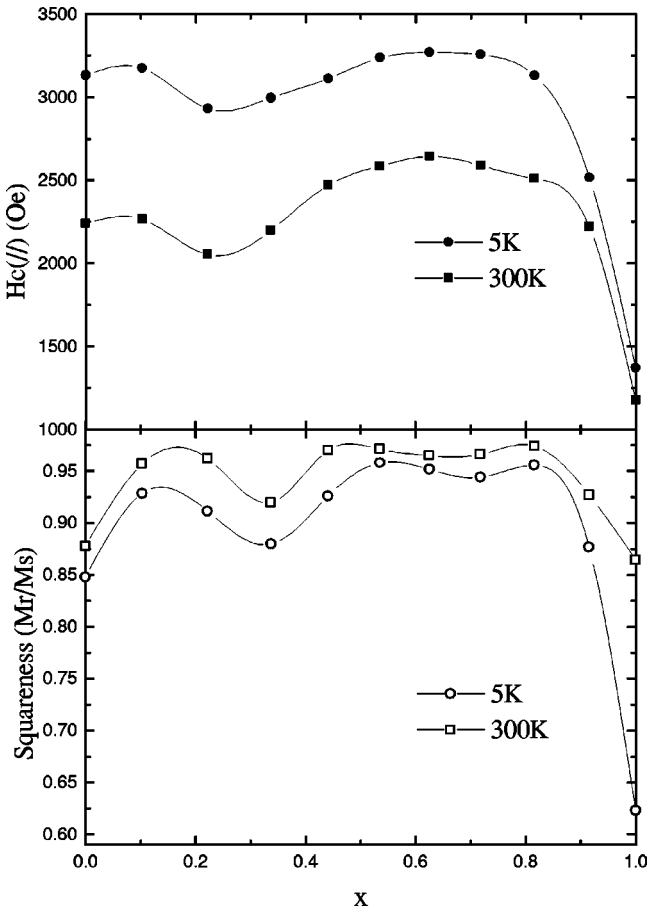

FIG. 7. The composition dependence of the coercivity and squareness ratio (M_r/M_s) of the arrays of $Fe_{1-x}Co_x$ nanowires at 300 and 5 K. The applied field is parallel to the nanowires.

and **H**($\perp$) indicate that the applied field is parallel or perpendicular to the nanowires. The hysteresis loops of the other samples are generally similar to these in shape, with some differences in the values of the coercive field, saturation magnetization, and remanence. Such hysteresis loops reveal that all arrays exhibit uniaxial magnetic anisotropy with the easy axis along the length of the nanowires. According to the XRD patterns, these easy axes are [110] and [1000] for bcc- and hcp-structured nanowires, respectively. However, for bulk Fe-Co alloys, the easy axes, due to the magnetocrystalline anisotropy, are along the [100] and [0001] directions, respectively, for the bcc and hcp structures. The shape of the nanowires (with aspect ratio ≈ 375) results in a very strong shape anisotropy, far higher in fact than the magnetocrystalline anisotropy, so that the easy axis orients along the nanowires.

Figure 7 shows the composition dependence of the coercivity and squareness (M_R/M_S) of the hysteresis loops for the $Fe_{1-x}Co_x$ AAO films with the field applied along the nanowires, at 300 and 5 K. With increasing Co concentration, the coercivity of the arrays of nanowires with the magnetic field parallel to the wires initially increases, reaches a maximum, and then decreases to a minimum around $x=0.22$. This tendency is attributed principally to the variation of the saturation magnetization of the $Fe_{1-x}Co_x$ nanowires; this will be discussed later in detail. Although the bulk Fe-Co alloy is a soft magnetic material, the coercive field of the arrays of $Fe_{1-x}Co_x$ nanowires (except $x=1.0$) with the applied field parallel to the nanowires is, due to shape anisotropy, larger than 2000 Oe. The squareness ratio at room temperature is above 0.92 for samples with $0.10 \leqslant x \leqslant 0.92$ with the applied field along the nanowires; this indicates that the arrays of $Fe_{1-x}Co_x$ nanowires have excellent perpendicular magnetic characteristics. The coercivity and squareness ratio of the pure Co AAO film are the lowest among the series of $Fe_{1-x}Co_x$ nanowires examined at both 300 and 5 K. This likely reflects the rather strong magnetocrystalline anisotropy in hcp Co nanowires. The magnetocrystalline anisotropy constant (K_1) of hcp Co is about 10 times that of other cubic Fe-Co alloys.[22] The magnetocrystalline anisotropy is also much stronger at low temperature and the axis of minimum magnetocrystalline energy is not along the length of the nanowires, so the squareness ratio of the $Fe_{1-x}Co_x$ nanowires at 5 is lower than that at 300 K.

It is well known that the remanent magnetization, coercivity, and shape of the hysteresis loop depend on the magnetization reversal process. Thus, in order to understand the high parallel coercivity of magnetic nanowires, it is important to investigate the magnetization reversal process in them. Each individual nanowire resembles a chain of spheres in shape, and arrays of nanowires exhibit uniaxial magnetic anisotropy. Thus the chains-of-spheres model appears well suited to interpret the magnetization reversal process in nanowires. Hereafter, we adopt this model in conjunction with parallel rotation and symmetric fanning mechanisms[16,17] to study the magnetization reversal process in magnetic nanowires. Each nanowire is assumed to be an ideal chain of single-domain spheres with uniaxial magnetic anisotropy. Each two adjacent spheres in the chain have only one contact point, so the spheres are magnetically isolated and the exchange interaction between spheres is consequently neglected. Further, the effect of magnetocrystalline anisotropy is not considered. With the above assumptions, using the chains-of-spheres model, the coercivity[16] of the nanowires for the parallel rotation mechanism is

$$H_C = \frac{\mu}{a^3} 6K_n = \pi M_S K_n . \tag{1}$$

In the case of symmetric fanning, the parallel coercivity[16] of the nanowires is

$$H_C = \frac{\mu}{a^3}(6K_n - 4L_n) = \frac{\pi M_S}{6}(6K_n - 4L_n), \tag{2}$$

where

$$L_n = \sum_{i=1}^{(n-1)/2 < i \leqslant (n+1)/2} \frac{n-(2i-1)}{n(2i-1)^3}, \tag{3}$$

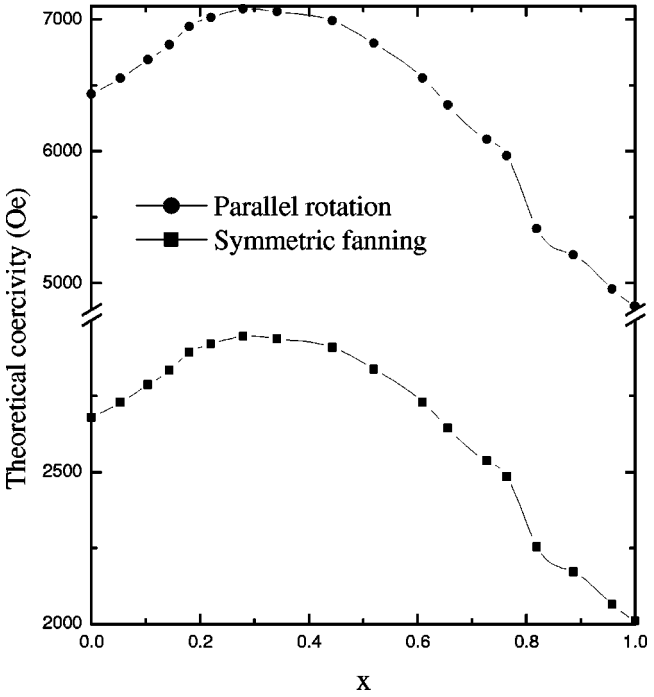

FIG. 8. The calculated coercivity of $Fe_{1-x}Co_x$ nanowires as a function of composition using the ''chains-of-spheres'' model in conjunction with the parallel rotation and symmetric fanning mechanisms.

$$M_n = \sum_{i=1}^{(n-2)/2<i\leqslant n/2} \frac{n-2i}{n(2i)^3}, \tag{4}$$

and

$$K_n = L_n + M_n = \sum_{i=1}^{n} \frac{n-i}{ni^3}. \tag{5}$$

Here μ is the dipole moment of a sphere, of diameter a, n is the number of the spheres in a nanowire, and M_S is the saturation magnetization of the nanowires.

The M_S value of bulk $Fe_{1-x}Co_x$ alloys[22] is used to approximate the M_S value of $Fe_{1-x}Co_x$ nanowires of the same composition. The diameter a is set at 20 nm because the average pore diameter is around 20 nm. The nanowire length is about 7.5 μm, so the number of spheres in a nanowire is equal to the aspect ratio ($n \approx 375$). Using the above parameters, we have calculated the coercivity of the $Fe_{1-x}Co_x$ nanowires for these two magnetization reversal mechanisms at room temperature. The results are shown in Fig. 8. The coercive fields predicted by the symmetric fanning mechanism agree roughly with the experimental results at 300 (Fig. 7). Deviations likely arise from the following factors that were neglected: (i) The interactions between the nanowires in the AAO film: these should cause a lower coercive field in comparison with that of a single nanowire.[7] (ii) The M_S of the Fe-Co nanowires was assumed to be equal to the M_S of the bulk alloys, since it could not be measured due to the technical reasons. However, the calculated results for the parallel rotation mechanism are far larger than the experimental values, with the total energy of the system calculated with the parallel rotation mechanism also being higher than that with the symmetric fanning mechanism. Thus the chains-of-spheres model with symmetric fanning, rather than parallel rotation, appears more appropriate to describe the magnetization reversal mechanism in these nanowires. Further, since all of the $Fe_{1-x}Co_x$ nanowires are uniform in geometry, then according to Eqs. (1) and (2), the coercivity of the $Fe_{1-x}Co_x$ nanowires should be proportional to the saturation magnetization. The coercivity variation with composition shown in Fig. 7 is generally similar to the variation of the saturation magnetization of bulk Fe-Co alloys with composition changes. However, around $x=0.22$, this correlation is broken, and the reasons for the drop in coercivity at this composition is unclear at the present time.

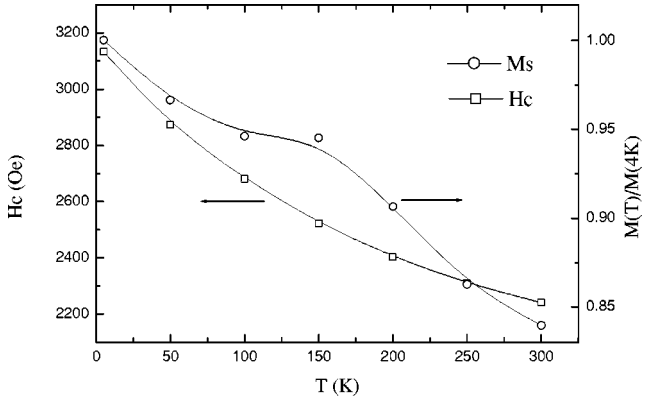

FIG. 9. The experimental coercivity and the relative saturation magnetization of the AAO films filled with Fe as a function of temperature.

As the saturation magnetization increases with decreasing temperature, then these same equations predict that the coercivity will increase with decreasing temperature. Figure 9 shows the experimental coercivity and the relative saturation magnetization of Fe nanowires in a self-assembled array with AAO film support as a function of temperature. There is again a general proportional relationship between the coercivity and saturation magnetization, although we suggest that the much stronger magnetocrystalline anisotropy at low temperature is the main factor responsible for the deviations from the predicted relationship.

IV. CONCLUSION

The $Fe_{1-x}Co_x$ nanowires in self-assembled arrays over the whole composition range have been successfully produced by the electrochemical method. By using several experimental techniques, the structure and magnetic properties of the arrays have been investigated. We find that all of the $Fe_{1-x}Co_x$ AAO films have an easy axis along the length of the nanowires, high coercivity, and high squareness ratio with the applied field parallel to the nanowires. This indicates that the AAO films filled with $Fe_{1-x}Co_x$ nanowires are promising candidates for high-density magnetic recording media. The theoretical coercivity of the $Fe_{1-x}Co_x$ nanowires

calculated by using the chains-of-spheres model with symmetric fanning agrees well with the experimental results.

ACKNOWLEDGMENTS

This work was supported by the National Natural Science Foundation of China, the Gansu Natural Science Foundation, the Key Teacher Foundation, and the Research Foundation for Scholars from Abroad, the latter two being divisions of the Ministry of Education P.R.C. One of the authors (Z.C.) would like to acknowledge the support provided by the Canadian International Development Agency during his recent visit to the University of Manitoba.

*Author to whom correspondence should be addressed. Electronic address: chenzy@lzu.edu.cn

[1] S. Dubois, J.M. Beuken, L. Piraux, J.L. Duvail, A. Fert, J.M. George, and J.L. Maurice, J. Magn. Magn. Mater. **165**, 30 (1997).
[2] L. Piraux, J.M. George, J.F. Despres, C. Leroy, E. Ferain, R. Legras, K. Ounadjela, and A. Fert, Appl. Phys. Lett. **65**, 2484 (1994).
[3] S.Y. Chou, Proc. IEEE **85**, 652 (1997).
[4] S. Charap, P.L. Lu, and Y. He, IEEE Trans. Magn. **33**, 978 (1997).
[5] R.M. Metzger, V.V. Konovalov, M. Sun, T. Xu, G. Zangari, B. Xu, M. Benakli, and W.D. Doyle, IEEE Trans. Magn. **36**, 30 (2000).
[6] Y. Peng, H.L. Zhang, S.L. Pan, and H.L. Li, J. Appl. Phys. **87**, 7405 (1999).
[7] J.M. Garcia, A. Asenjo, J. Velazquez, D. Garcia, M. Vazquez, P. Aranda, and E. Ruiz-Hitzky, J. Appl. Phys. **85**, 5480 (1999).
[8] L. Sun, P.C. Searson, and C.L. Chien, Appl. Phys. Lett. **74**, 2803 (1999).
[9] L. Sun, P.C. Searson, and C.L. Chien, Phys. Rev. B **61**, R6463 (2000).
[10] A.O. Adeyeye, R.P. Cowburn, and M.E. Welland, J. Magn. Magn. Mater. **213**, L1 (2000).
[11] S. Kawai and R. Ueda, J. Electrochem. Soc. **122**, 32 (1975).
[12] Z. Turgut, J.H. Scott, M.Q. Huang, S.A. Majetich, and M.E. McHenry, J. Appl. Phys. **83**, 6468 (1998).
[13] R.H. Yu, L. Ren, S. Basu, K.M. Unruh, A. Parvizi-Majidi, and J.Q. Xiao, J. Appl. Phys. **87**, 5840 (2000).
[14] J.I. Martin, J. Nogues, I.K. Schuller, M.J. Van Bael, K. Temst, C. Van Haesendonck, V.V. Moshchalkov, and Y. Bruynseraede, Appl. Phys. Lett. **72**, 255 (1998).
[15] L. Zhang and A. Manthiram, Phys. Rev. B **54**, 3462 (1996).
[16] I.S. Jacobs and C.P. Bean, Phys. Rev. **100**, 1060 (1955).
[17] I.S. Jacobs and F.E. Luborsky, J. Appl. Phys. **28**, 467 (1957).
[18] W.F. Brown, Jr., Ann. (N.Y.) Acad. Sci. **147**, 461 (1969).
[19] E.M. Kakuno, D.H. Mosca, I. Mazzaro, N. Mattoso, W.H. Schreiner, and M.A.B. Gomes, J. Electrochem. Soc. **144**, 3222 (1997).
[20] W.C. Ellis and E.S. Greiner, Trans. Am. Soc. Met. **29**, 415 (1941).
[21] O. Kitakami, H. Sato, Y. Shimada, F. Sato, and M. Tanaka, Phys. Rev. B **56**, 13 849 (1997).
[22] E. P. Wohlfarth *et al.*, *Ferromagnetic Materials* (North-Holland, Amsterdam, 1980), Vols. 1 and 2.